GMAW-P 频率-特性复合弧长适应控制法

华学明[1]， 李 芳[1]， 陆志强[1]， 吴毅雄[1,2]

（1. 上海交通大学 上海市激光制造与材料表面改性重点实验室，上海 200240；
2. 上海交通大学 金属基复合材料国家重点实验室，上海 200240）

华学明

摘 要：为了提高 GMAW-P 焊接弧长控制的调节速度，减少弧长调节过程中脉冲频率、焊接电流的波动范围，提出了基于 DSP 数字控制脉冲熔化极气体保护焊接电源采用频率－特性复合弧长适应控制法．在焊接过程中通过实时采集电弧电压信号、焊接电流信号，当弧长发生扰动时，在当前脉冲周期内，以基值时间和给定电压为控制量，从而保证在弧长调节过程中脉冲频率的变化较小．台阶试验和爬坡试验表明，此控制方法的弧长调节过程快速、稳定，焊接电流、脉冲频率波动范围小，焊机具有良好的弧长调节性能．

关键词：脉冲熔化极气体保护焊；弧长控制；焊接电源

中图分类号：TG444 文献标识码：A 文章编号：0253－360X(2009)10－0053－04

0 序 言

目前，脉冲熔化极气体保护焊(GMAW-P)是一种重要的焊接方法，在航天航空、造船等领域有着广泛的应用[1]．GMAW-P 的熔滴过渡过程的稳定性是获得优质焊接质量的保证，一般以一脉一滴的过渡方式为主[2]．国内外学者对 GMAW-P 展开了大量的研究工作，并且取得了一些研究成果．但由于 GMAW-P 焊接过程中，脉冲电流波形不断地在基值与峰值电流之间进行切换，因此弧长也在两个值之间不断变化，很容易出现导电嘴的回烧．如何有效快速调节控制电弧长度是 GMAW-P 亟待解决的工艺问题之一．针对 GMAW-P 电弧长度的控制方法，文中提出了一种新型频率-特性复合 GMAW-P 弧长适应控制方法．

1 GMAW-P 过程控制

GMAW-P 焊接过程主要的 2 个问题是熔滴过渡控制和弧长控制．熔滴过渡控制通过经验公式 $I_p^n \times t_p = C$（n 和 C 为常数）即选择合适的脉冲电流、脉冲时间匹配达到最佳的一脉一滴熔滴过渡焊接[3]．

基值电流 I_b 的作用是在峰值电流停歇期间维持焊丝与熔池之间的导电状态，维持电弧．基值电流是调节平均焊接电流和调节焊接热输入的重要工艺参数，对于低碳钢基值电流的范围为 30～50 A 较为合适[4]．因此，弧长控制可以采用控制基值时间，即改变脉冲频率的方式获得．

但脉冲频率与熔滴过渡频率以及熔滴的体积有着重要的关系[3]．在一定的送丝速度下，为保证实现一脉一滴的熔滴过渡方式，必定存在一个最佳匹配脉冲频率．因此为保证一脉一滴的熔滴过渡方式，焊接过程中脉冲频率的波动应尽可能小．

焊接过程中弧长受各种干扰而变化．下面分析由导电嘴到工件的距离(CTWD)变化引起弧长变化时，分别在平特性与下降特性焊接电源时所引起的脉冲参数的波动．

如图 1 所示，对于始终保持平特性的焊接电源特性，当弧长从 $l_1 \rightarrow l_2$ 时，电弧的稳定工作点从 A_0 点移到 A_2 点．平均焊接电流变化从 $I_0 \rightarrow I_2$，焊接电流变化 ΔI_2；脉冲频率变化 Δf_2．

若电源外特性为缓降特性时，如图 1 中外特性曲线 2．当弧长从 $l_1 \rightarrow l_2$，电弧的稳定工作点从 A_0 点移到 A_1 点．电流变化从 $I_0 \rightarrow I_1$，焊接电流变化 ΔI_1；脉冲频率变化 Δf_1．

从上面分析可知，若焊接电源为平特性，即仅调节基值时间 t_b 改变脉冲频率控制电弧长度，当弧长波动后达到新的稳定工作点时，引起焊接电流的波动较大．如果能同时对 GMAW-P 焊接过程中的外特性以及脉冲频率进行控制，当弧长发生波动时，电流

收稿日期：2008－07－14

的静态误差小. 文中对此提出了一种频率-特性复合GMAW-P 弧长适应控制方法.

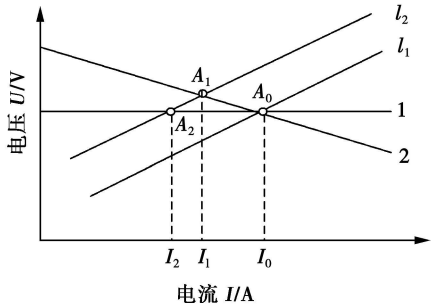

图 1 电源—电弧系统的静态平衡关系

Fig. 1 Static balance between power source and arc system

2 频率-特性复合弧长适应控制

2.1 频率-特性复合弧长适应控制思想

设计双变量弧长控制器, 一方面通过基值时间 t_b 来调节脉冲频率使弧长保持稳定; 同时, 控制焊接电源的外特性, 实时修正 u_g 以保证脉冲频率在小范围内波动. 通过实时计算每个脉冲周期中的反馈电压与给定电压值比较, 来调整熔化速度, 使每个脉冲周期中的平均电压与给定电压相等, 从而在导电嘴高度发生变化等扰动情况下, 弧长在一段时间的调节后得到快速恢复.

2.2 弧长信号采样与离散优化处理算法

系统采用离散采样求积分的方法处理每个脉冲周期的瞬时弧长, 其特点是: 采用每个周期的电弧电压积分作为弧长信号, 减小随机瞬时电压扰动所带来的误差. 控制目标是每一个脉冲周期的"瞬时弧长", 即保证每个脉冲周期的平均电压与给定电压相等. 如图 2 所示, 图中 1, 2 所示两部分的面积相等即表示每个脉冲周期的平均电压与给定电压相等. 由此可见, 用"面积"即"积分"的概念也完全可以表示出每个脉冲周期的瞬时弧长. 对于数字控制系统, 积分可以由离散累加和得到, 计算方便简单, 不会因为计算而带来附加误差.

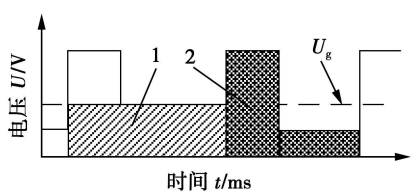

图 2 电弧电压积分处理

Fig. 2 Integral of arc voltage

具体弧长积分信号优化处理过程如下.

在每一个脉冲周期开始时作为一个新的控制周期的起点, 每隔一定的时间间隔(采样周期 T_c)采样一次电压, 并与前一次的采样值累加; 同时, 累加给定电压值. 并且, 比较采样电压累加和与给定电压累加和, 当满足条件式(2)时, 基值电流切换到峰值电流, 开始新的脉冲周期.

$$\left.\begin{aligned} U_{\mathrm{fadd}}(n) &= U_{\mathrm{fadd}}(n-1)+U_{\mathrm{f}}(n)=\sum_{i=1}^{n}U_{\mathrm{f}}(i) \\ U_{\mathrm{gadd}}(n) &= \sum_{i=1}^{n}U_{\mathrm{g}}(i) \end{aligned}\right\} \quad (1)$$

$$\sum_{i=1}^{n}U_{\mathrm{f}}(i)\leqslant\sum_{i=1}^{n}U_{\mathrm{g}}(i) \quad (2)$$

2.3 频率-特性复合控制器调节过程

频率-特性复合弧长控制原理是: 监控每个脉冲周期的平均电流变化, 根据平均电流的大小实时优化电压给定值. 当弧长变化时, 通过调整焊接电源的外特性, 使得给定电压与给定电流联动, 随着焊接平均电流的变化而优化电压的设定, 从而保证系统在全电流范围内具有良好的电弧动态响应性能.

当弧长为 l_0 时, 工作点为 A_0, 对应的给定值为 (I_g, U_g). 若受到干扰因素的影响, 弧长变短为 l_1, 工作点移至 A_1 (I_1, U_1)(图 3).

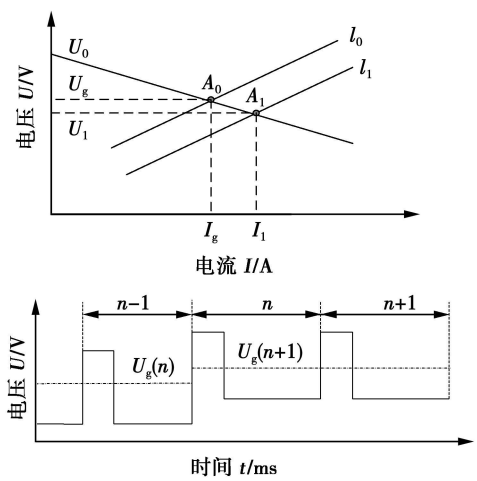

图 3 频率-特性复合控制器原理图

Fig. 3 Frequency-character combine controller

调节过程如下.

(1) 根据设定的平均电流和平均电压, 确定工作点 A_0(I_g, U_g).

(2) 根据平均电流确定外特性的斜率 k.

(3) 外特性计算公式为

$$U(n+1)=U(n)+k[I_g-I(n)] \quad (3)$$

式中: $I(n)$为第 n 个脉冲周期中计算的反馈平均电流; $U(n)$为第 n 个脉冲周期中的给定电压值; $U(n+1)$为下一个脉冲周期$(n+1)$中平均电流发生偏移后新给定电压.

(4) 在得到新的给定电压后, 通过实时的电压反馈式(1)确定基值时间 t_b, 当反馈的平均电压与给定电压相等时, 如式(2)所示, 电流波形由基值切换到峰值, 开始一个新的脉冲周期.

3　弧长适应控制工艺试验与分析

为试验弧长调节性能分别进行台阶和斜坡试验. 试验条件: 保护气体为 100%氩气, 流量为 15 L/min, ϕ 1.2 mm 低碳钢焊丝, 送丝速度为 4 m/min, 焊接速度 v_w 为 30 cm/min, 初始导电嘴到工件的距离 $h_1=20$ mm (图 4), 台阶高度 $h_2=5$ mm, 斜坡初始距离水平面的垂直距离 $h_3=5$ mm; 升至斜坡顶部时距离水平面的垂直距离 h_4 为 10 mm, 电信号采样频率为 20 kHz.

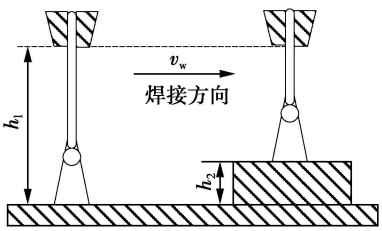

图 4　台阶试验示意图

Fig. 4　Sketch of step experiment

3.1　台阶试验

图4 为台阶试验示意图. 针对单变量弧长控制(即仅 t_b 作为控制量)与频率-特性复合弧长控制法分别试验, 具体的试验数据及分析如下.

采用单变量弧长控制方法, 在台阶附近, 从 A 点到 B 点为调节过程, 调节时间为 0.90 s, 如图 5a 所示. 在台阶前后平均电流的变化从 105.53 A→120.74 A, 变化了 14.4%; 脉冲频率从 83.60 Hz→101.20 Hz, 变化21%. 而采用频率-特性复合弧长控制方法, 系统的调节过程为从图 5b 中的 C 点到 D 点, 仅为 0.17 s. 在台阶前后平均电流的变化从 111.21 A→116.98 A, 变化 5.18%; 脉冲频率从 87.35 Hz→93.66 Hz, 变化 7.22%. 从图 6 中可知频率-特性复合控制法弧长调节频率和电流变化比单变量控制法小.

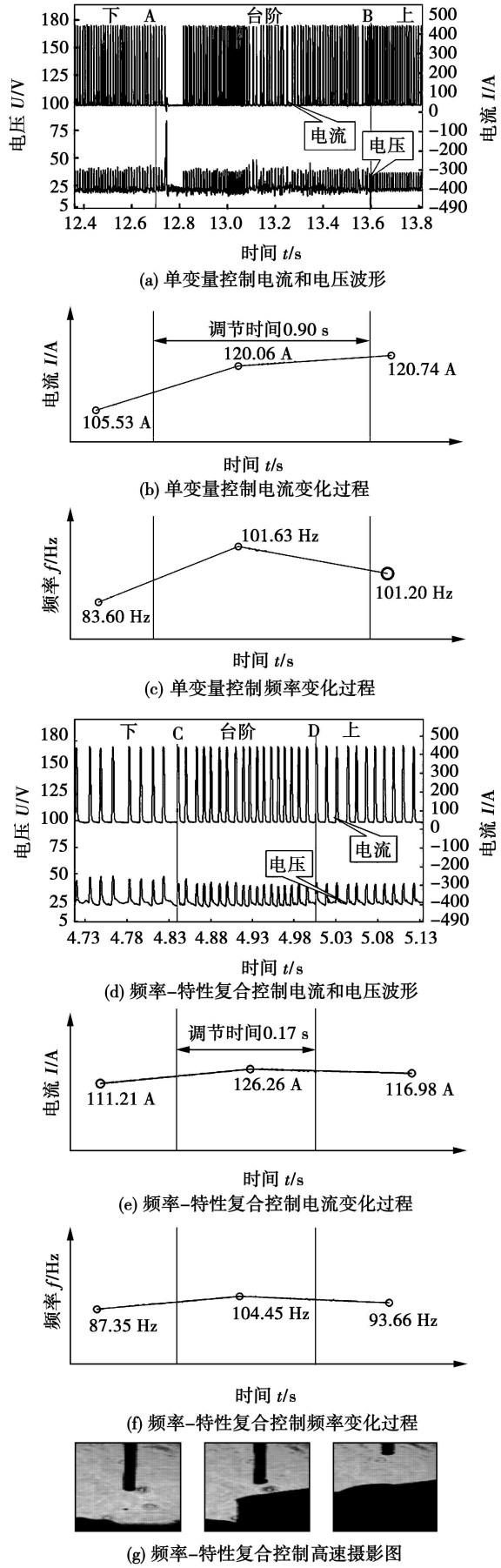

图 5　台阶试验电流、电压波形及高速摄影图

Fig. 5　Waveform of step experiment

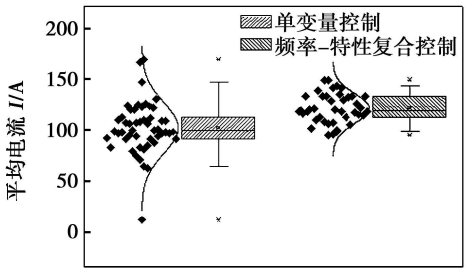

(a) 两种弧长控制方法平均电流对比

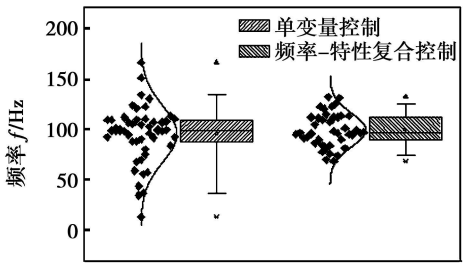

(b) 两种弧长控制方法脉冲频率对比

图 6 台阶试验调节过程

Fig. 6 Adjust process for step experiment

3.2 斜坡试验

图 7 为斜坡试验示意图, 斜坡初始距离水平面的垂直距离为 5 mm; 升至斜坡顶部时距离水平面的垂直距离为 10 mm. 图 8a, b 分别为斜坡试验中斜坡底部和顶部截取的电流和电压波形. 斜坡试验焊接过程非常稳定, 无飞溅, 无短路, 熔滴过渡正常均匀. 在整个的爬坡过程中, 平均电流总体变化仅为 5 A, 波动率为 4.4%, 而脉冲频率的波动仅为 6.8%.

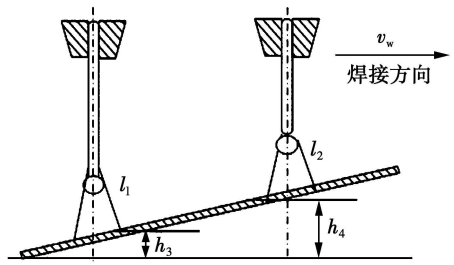

图 7 斜坡试验示意图

Fig. 7 Sketch of slope experiment

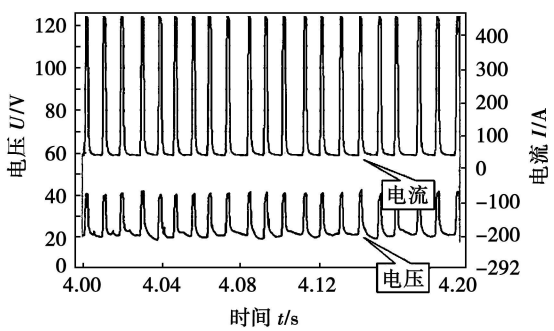

(a) 斜坡底部

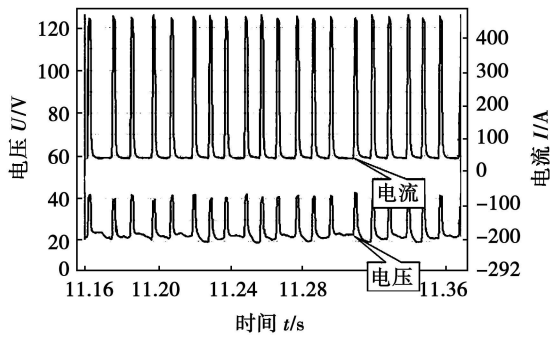

(b) 斜坡顶部

图 8 斜坡试验实测波形

Fig. 8 Waveform of slope experiment

4 结 论

针对 GMAW-P 焊接的特点, 对 GMAW-P 弧长适应控制展开研究, 设计了频率-特性复合弧长控制器. 当弧长发生变化时, 一方面通过基值时间(脉冲频率)控制使弧长保持稳定, 同时, 控制焊接电源的外特性即根据焊接电流的变化改变电弧电压的给定值, 从而保证在弧长调节过程中脉冲频率的变化较小. 台阶试验和爬坡试验表明, 此控制方法的调节过程快速、稳定, 焊接电流变化小、脉冲频率变化小.

参考文献:

[1] 中国机械工程学会焊接学会. 焊接手册: 第 1 卷[M]. 北京: 机械工业出版社, 1992.

[2] 蒙永民, 黄石生, 薛家祥, 等. GMAW-P 焊熔滴过渡及其控制的研究现状与发展[J]. 电焊机, 2000, 30(1): 1—5.
Meng Yongmin, Huang Shisheng, Xue Jiaxiang, *et al*. The situation and development of metal transfer and its control in GMAW-P [J]. Electric Welding Machine, 2000, 30(1): 1—5.

[3] Palani P K, Murugan N. Selection of parameter of pulsed current gas metal arc welding[J]. Journal of Materials Processing Technology, 2006, 172(1): 1—10.

[4] Collard J F. Adaptive pulsed GMAW control: the digital pulse system [J]. Welding Journal, 1988, 67(11): 35—38.

作者简介: 华学明, 1965 年 7 月出生, 博士, 副教授. 主要从事数字化焊接电源、高效焊接和焊接过程智能控制等方面研究. 发表论文 40 余篇.

Email: xmhua@sjtu.edu.cn

grains in HAZ become coarse, and the grain boundary melting occurs. Under the condition of 23 kA welding current, 8-cycle welding time and 4.5 kN electrode force, the cellular-dendritic structure at the edge of the nugget is refined, and the equiaxed dendritic structure in the central portion of the nugget tends to be changed into the equiaxed grains without secondary axis of crystal with average grain size of 12.96 μm.

Key words: magnesium alloy; resistance spot welding; microstructure

Image processing algorithm for weld seam recognition based on color analyzing ZOU Yirong, WU Zheming, GUO Guilin, DU Dong (Key Laboratory for Advanced Materials Processing Technology Ministry of Education, Tsinghua University, Beijing 100084, China). p 37—40

Abstract: An algorithm of weld seam recognition based on color analyzing is proposed for automatic welding and automatic nondestructive test technologies. Based on color theory and the principles of image segmentation, the image representation in RGB (red, green and blue) color space is studied, and the method of color space transformation is proposed. The experiments demonstrate that the image described in the newly defined color space is able to be segmented by threshold value, which allows the seam region to be located and makes the algorithm and recognition easy.

Key words: image color; RGB color space; weld seam recognition; image processing

Influence of cerium oxide on mechanical properties of low alloy steel electrode GUO Yonghuan, FAN Xiying, WANG Guangfeng (College of Mechanical and Electrical Engineering, Xuzhou Normal University, Xuzhou 221116, China). p 41—44

Abstract: Micro-amount cerium oxide was transferred into the electrode coating of low alloy steel in the experiment, and the formula of mechanical property quantitative relationship between cerium oxide and deposited metal was obtained by calculating and curve fitting in MATLAB function. The results show that the tensile strength error decreases from 44 MPa calculated with empirical formula to 1 MPa with the quantitative formula, and the lower yield strength error from 100 MPa to 2 MPa. The rare-earth quantity can be converted to carbon equivalent and introduced into the quantitative formula as a parameter, which makes the test times and the cost of electrode design reduce.

Key words: cerium oxide; low alloy steel electrode; mechanical properties; quantitative relationship

Shear strength and fracture surface analysis of BiAgNiCuGe/Cu joint MENG Gongge, LI Zhengping (School of Material Science and Engineering, Harbin University of Science and Technology, Harbin 150040, China). p 45—48

Abstract: The microstructure, joint shear strength and fracture surface of high-temperature lead-free solder Bi-*x*Ag-0.4Ni-0.2Cu-0.1Ge (x=2, 5, 8, 11, 14) were analyzed with scanning electron microscopy, energy dispersive X-ray spectrometry and electronic tensile testing machine. The results show that interface microstructure mainly consists of primary Ag, primary crystal Bi, eutectic phase and little $NiBi_3$ phase. With the increasing of Ag in solder, primary Ag increases gradually and shear strength heightens obviously. No intermetallic compound forms between solder and Cu substrate, which join mainly through the diffusion of liquid solder atoms to Cu crystal boundaries. The diffusion of Bi to Cu crystal boundary is more than that of Ag. The interface between solder and Cu substrate is the weak region of joint and is shear fracture starting point.

Key words: microstructure; shear strength; fracture surface; high-temperature lead-free solder; BiAgNiCuGe

Automatic extraction of locating data for bulk defects in I-shaped laser weldments SHI Duanhu[1], GANG Tie[2], YANG Genxi[1], HUANG Chuanhui[1] (1. School of Electromechanical Engineering, Xuzhou Institute of Technology, Xuzhou 221008, China; 2. State Key Laboratory of Advanced Welding Production Technology, Harbin Institute of Technology, Harbin 150001, China). p 49—52

Abstract: In order to determine the spatial position of bulk defects in I-shaped weldments, multiple-view method was adopted to test it nondestructively. Mathematic models of small defect depth and deviation for laser weldments with I style were established, and the depth and deviation of small defects in precision weld were determined. Theoretical analysis was preceded on factors, which can influence the locating precision of small defects, and the main influencing factors were obtained. In order to achieve the rapid detection of laser weldments and improve the robust of detection, automatic extraction algorithm of defect projection distance was put forward on the basis of defects segmentation and thinning, and algorithm verification was carried out by using the method of simulation defect. Experimental results show that the extracted method in this paper is feasible.

Key words: I-shaped laser weldments; X-ray image; projection distance; automated extraction

Frequency-character combine control method of arc length adjustment of GMAW-P HUA Xuemin[1], LI Fang[1], LU Zhiqiang[1], WU Yixiong[1,2] (1. Shanghai Key Laboratory of Materials Laser Processing and Modification, Shanghai Jiaotong University, Shanghai 200240, China; 2. State Key Laboratory of Metal Matrix Composite, Shanghai Jiaotong University, Shanghai, 200240, China). p 53—56

Abstract: In order to decrease fluctuating of pulse frequency and welding current while adjusting arc length, the frequency-character combine controller of arc length adjustment was researched and designed in GMAW-P welding machine based on digital signal process controlling. Base time and welding voltage setting were used as controlling variables in order to ensure pulse frequency within small

change during arc length adjustment. The experiments show that this control method of arc length adjustment has the characteristics of fast adjusting and good stability; welding current, pulse frequency can change smaller when arc length is disturbed.

Key words: pulse gas metal arc welding; arc length control; welding machine

Finite element analysis on soldered joint reliability of QFN device JI Feng, XUE Songbai, ZHANG Liang, WANG Hui (College of Materials Science and Technology, Nanjing University of Aeronautics and Astronautics, Nanjing 210016, China). p 57—60

Abstract: Quarter models of QFN (quad flat non-leaded) were set-up by means of ANSYS software, Anand model was used to establish the constitutive equation of Sn3.0Ag0.5Cu solder, and the reliability of QFN with different solder joint shape was presented. The results indicate that the maximum value of stress is at the package corner, which value change is cyclical and additive. The solder joint reliability of leads with pullback design is poorer than that of the leads non-pullback design that cannot influence the value of plastic work caused by the solder fillet length and land length significantly. The effect of solder thickness is very obviously, and the average plastic work is inversely proportional to solder thickness. The area of center pad soldering has considerable effect to the solder joint reliability, and the size of the area could be increased appropriately in the reflow soldering process.

Key words: finite element simulation; reliability; solder joint shape; plastic work

Mechanical properties of soldered joints of QFP devices SHENG Zhong, XUE Songbai, ZHANG Liang, GAO Lili (College of Materials Science and Technology, Nanjing University of Aeronautics and Astronautics, Nanjing 210016, China). p 61—64

Abstract: Mechanical properties of soldered joints of quad flat packge (QFP) devices are investigated by numerical simulation, and the results of simulation indicate that soldered joints of high density in leads and the lead-free exhibit lower equivalent stress. The results of experiment indicate that the tensile strength of SnAgCu soldered joints is significantly greater than that of SnPb soldered joints, and the tensile strength of devices soldered by laser reflow increases by 25% than that by infrared reflow. The fracture microstructure of QFP for SnPb solder is coarse, but for SnAgCu solder is fine. The dimples in the fracture of joints formed by infrared reflow welding are not uniform, which the fracture includes brittle fracture and toughness fracture; but those by laser soldering are uniform, which fracture is toughness fracture. The experiment results are close to the simulated result.

Key words: finite element; quad flat packge devices; mechanical properties; microstructure

Mechanical properties of brazing joint of alumina ceramics to mild steel LI Zhuoran, FAN Jianxin, FENG Jicai (State Key Laboratory of Advanced Welding Production Technology, Harbin Institute of Technology, Harbin 150001, China). p 65—67, 72

Abstract: The shear strength of alumina ceramic/AgCuTi/mild steel brazed joint was tested to evaluate the mechanical property of the joint. Effect of processing parameters including brazing temperature and holding time on the joint mechanical property was also discussed with scanning electron microscopy and energy dispersive spectroscopy. Results showed the maximum shear strength was 103 MPa, which was achieved when the brazing temperature was 900 ℃ and holding time was 5 min. In this case, fracture happened mainly at the alumina ceramic/brazing alloy interface and partly at Al_2O_3, TiMn and $TiFe_2$ intermetallic compounds.

Key words: alumina ceramic; active metal brazing; shear strength

Microstructure and mechanical properties of friction stir welding joints of Al-Zn-Mg-Sc-Zr Alloy CHEN Jiqiang[1], YIN Zhimin[1], HE Zhenbo[1,2], PENG Yongyi[1] (1. School of Materials Science and Engineering, Central South University, Changsha, 410083, China; 2. Northeast Light Alloy Co., Ltd., Harbin 150060, China). p 68—72

Abstract: The joints of friction stir welding of Al-Zn-Mg-Sc-Zr alloy were investigated, and the mechanical properties and microstructures of the joint were analysed. The results show that the distribution of micro-hardness in the cross-section presents a trend of high-low-high-low-high, the maximal hardness appears in the region of the weld nugget and the lowest hardness in head-affected zone (HAZ), and the welding coefficient reaches 0.90. The weld nugget has a dynamic recrystallized fine isometric crystal structure with the size of 1-2 μm, and the precipitation phases in the base metal are melted and broken up to small round particles; the thermo-mechanically affected zone has a highly curved structure, and the precipitation phases transform to club-shaped; the size of grains in HAZ is larger than that in the base metal. The tensile samples of welding joint break in the HAZ.

Key words: Al-Zn-Mg-Sc-Zr alloy; friction stir welding; welded joint; microstructure; mechanical properties

Structure and property of Fe-base manual SHS welding joint XIN Wentong[1,2], MA Shining[1], LI Zhizun[2], LI Baofeng[2] (1. National Key Laboratory for Remanufacturing, Armored Force Engineering Academy, Beijing 100072, China; 2. Base Department, Ordnance Engineering College, Shijiazhuang 050003, China). p 73—75

Abstract: In order to solve a problem of the low mechanical properties of manual SHS (self-propagating high-temperature synthesis) welding joint, a new iron-base manual SHS welding material was developed by adding iron alloy materials and CuO+Al and Fe_2O_3+Al as the thermit, and the structure and properties of the welded joint were studied. The results indicate that the welding is fusion welding, and weld appearance is good. Cu-Fe alloy in the molten pool experiences liquid phase separation during rapid solidification,